Ocean Sci., 11, 187–194, 2015
www.ocean-sci.net/11/187/2015/
doi:10.5194/os-11-187-2015

Ocean Science
Open Access

Roles of initial ocean surface and subsurface states on successfully predicting 2006–2007 El Niño with an intermediate coupled model

F. Zheng and J. Zhu

International Center for Climate and Environment Science (ICCES), Institute of Atmospheric Physics, Chinese Academy of Sciences, Beijing 100029, China

Correspondence to: F. Zheng (zhengfei@mail.iap.ac.cn)

Received: 28 April 2014 – Published in Ocean Sci. Discuss.: 19 June 2014
Revised: 25 October 2014 – Accepted: 6 January 2015 – Published: 6 February 2015

Abstract. The 2006–2007 El Niño event, an unusually weak event, was predicted by most models only after the warming in the eastern Pacific had commenced. In this study, on the basis of an El Niño prediction system, roles of the initial ocean surface and subsurface states on predicting the 2006–2007 El Niño event are investigated to determine conditions favorable for predicting El Niño growth and are isolated in three sets of hindcast experiments. The hindcast is initialized through assimilation of only the sea surface temperature (SST) observations to optimize the initial surface condition, only the sea level (SL) data to update the initial subsurface state, or both the SST and SL data. Results highlight that the hindcasts with three different initial states can all successfully predict the 2006–2007 El Niño event 1 year in advance and that the hindcast initialized by both the SST and SL data performs best. A comparison between the various sets of hindcast results further demonstrates that successful prediction is more significantly affected by the initial subsurface state than by the initial surface condition. The accurate initial surface state can trigger the easier prediction of the 2006–2007 El Niño, whereas a more reasonable initial subsurface state can contribute to improving the prediction in the growth of the warm event.

1 Introduction

El Niño–Southern Oscillation (ENSO), which is one of the most striking interannual variabilities in the tropical Pacific Ocean, has been studied for several decades. Understanding the changes in its characteristics remains an important issue for worldwide environmental and socioeconomic interests (McPhaden et al., 2006; Ashok and Yamagata, 2009). During the past 2–3 decades, ENSO forecasts have made remarkable progress, reaching a stage in which skillful predictions can be made 6–12 months in advance. Many climate models from operational centers have routinely been used to make ENSO predictions in real time (Latif et al., 1998; Kirtman et al., 2002), although the skill of sea surface temperature (SST) forecasts in the equatorial Pacific is strongly model dependent and widely divergent across various prediction systems (Jin et al., 2008; Barnston et al., 2012). To improve the prediction skills, intensive effort has been made in both model improvements and better constraint of initial conditions. The latter is particularly important in the ocean because the memory for ENSO resides in the ocean (e.g., Neelin et al., 1998), and the importance of ocean data in making ENSO predictions has been demonstrated in a number of studies (e.g., Ji and Leetmaa, 1997; Ji et al., 2000; Alves et al., 2004; Keenlyside et al., 2005; Zheng et al., 2006, 2007; Zheng and Zhu, 2008; Yang et al., 2010; Zhu et al., 2012).

However, as demonstrated by Barnston et al. (2012), an apparent retrogression in skill exists for ENSO predictions in the 2002–2011 study period, compared with those in the 1981–2010 period, and the real-time ENSO prediction skill of models in the past decade is significantly lower than that of the less-advanced models of the 1980s and 1990s. For example, the 9-year sliding correlation for the hindcasts during the 1981–2010 period has an average score of 0.65 at a 6-month lead time, but the prediction skill of the correlation decreases to 0.42 for the 2002–2011 period (Barnston et al., 2012). Specifically, in the case of the 2006–2007 El Niño event, which was unusually weak (Hackert et al., 2007; McPhaden, 2008; Yang et al., 2010), most seasonal climate forecasts

from operational centers only predicted the event after the warming had already become apparent and was basinwide (McPhaden, 2008). The composite forecast for December 2006 from the International Research Institute for Climate Prediction (IRI) indicates that the warm anomaly was underpredicted by more than 0.5 °C. (A review of forecast skills is available on the IRI website at http://iri.columbia.edu.)

The limited predictability may be attributed to factors such as errors in the oceanic initial conditions, state-dependent stochastic forcing, or model errors (Palmer, 2001). In this study, we investigated possible improvements in predicting this warm event by focusing on the role of the oceanic initial states. On the basis of the ensemble Kalman filter (EnKF) algorithm (e.g., Evensen, 2009), the roles of the initial ocean surface and subsurface states on the 2006–2007 El Niño predictions were examined in three sets of retrospective forecast experiments. In the first set, only the SST data was assimilated to provide accurate surface initial conditions, whereas only sea level (SL) data was assimilated to provide the updated information of the subsurface water temperature entrained into the mixed layer in the model. In the third set, both SST and SL data were assimilated. The forecast differences in the three sets of the retrospective experiments with initializations by the three separate data assimilation schemes were then examined to isolate the effects of the various initial states on predicting the warm event.

2 Model and initialization schemes

In this section, we briefly describe the model components and the designs of three initialization schemes on the basis of the EnKF algorithm.

2.1 Description of the model components

The ENSO-coupled model we used here is an intermediate coupled model (ICM) that was first developed by Keenlyside and Kleeman (2002) and Zhang et al. (2005); various components of the ICM are briefly described here (Fig. 1). Its ocean dynamical component consists of both linear and nonlinear components. The former was essentially a McCreary-type (1981) modal model but was extended to include horizontally varying background stratification. Different from the commonly used Zebiak–Cane model (1987), this ICM considers the realistic vertical structure of the upper ocean, spatially varying stratification, and partial nonlinear effects. For example, when 10 vertical modes are included in the calculation of dynamic ocean fields, along with a parameterization of the local Ekman-driven upwelling, this model yields realistic simulations of the mean equatorial circulation and its variability in the tropical Pacific (Keenlyside and Kleeman, 2002).

The ocean model domain extends from 33.5° S to 33.5° N and from 124° E to 70° W, covering the tropical Pacific basin

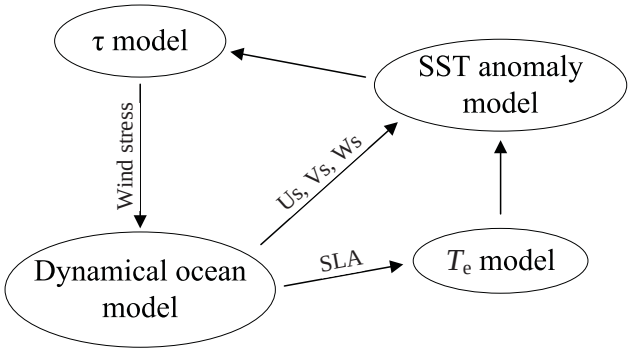

Figure 1. A schematic illustrating the ICM consisting of a dynamical ocean model, an SST anomaly model with an empirical parameterization for T_e in terms of SLA, and a statistical atmospheric wind stress (τ) model. Adopted from Zhang et al. (2005).

with a realistic representation of continents. The model has a 2° zonal grid spacing and a meridional grid stretching from 0.5° within 10° of the Equator to 3° at the northern and southern boundaries. Vertically, a 5500 m flat-bottom ocean is assumed; the linear component has 33 levels, chosen as in Levitus (1982), with 8 levels in the upper 125 m. The two layers used to simulate the nonlinear effects and high-order baroclinic modes span the upper 125 m and are divided by a surface mixed layer whose depth is prescribed from observations (Monterey and Levitus, 1997).

An SST anomaly model is embedded within this dynamical framework. The governing equation (i.e., Eq. 1) describes the evolution of surface mixed layer temperature anomalies, driven by ocean horizontal advection and entrainment associated with both specified mean and simulated anomalous currents.

$$\begin{aligned}\frac{\partial T'}{\partial t} = & -u'\frac{\partial \overline{T}}{\partial x} - (\overline{U}+u')\frac{\partial T'}{\partial x} - v'\frac{\partial \overline{T}}{\partial y} - (\overline{V}+v')\frac{\partial T'}{\partial y} \\ & - \left\{(\overline{W}+w')M(-\overline{W}-w') - \overline{W}M(-\overline{W})\right\}\frac{\overline{T_e}-\overline{T}}{H}, \\ & -(\overline{W}+w')M(-\overline{W}-w')\frac{T'_e-T'}{H} \\ & +\frac{\kappa_h}{H}\nabla_h(H\nabla_h T') + \frac{2\kappa_v}{H(H+H_2)}(T'_e - T') - \alpha T'\end{aligned} \quad (1)$$

where, T' and T'_e are anomalies of SST and the temperature of subsurface water entrained into the mixed layer; u', v' and w' are anomalies of ocean currents (horizontal and vertical) in the surface mixed layer; H is the depth of the mixed layer; H_2 is a constant (125 m); $M(x)$ is the Heaviside function; κ_h and κ_v are horizontal diffusion and vertical mixing parameters, respectively; and other variables are mean climatology fields. The surface heat flux is parameterized as being negatively proportional to local SST anomalies. These components are used to calculate SST changes from the equation given above.

As demonstrated by Zhang et al. (2005), having a realistic parameterization for the temperature of the subsurface water entrained into the mixed layer (T_e) is crucial to the performance of SST simulations in the equatorial Pacific. Based on

the empirical orthogonal function (EOF) method, an empirical T_e model was constructed from a historical relationship between the interannual variations in T_e and SL during the period 1963–1996 and was demonstrated to be effective in improving the SST simulations. The ocean model is coupled with a statistical atmospheric model, which specifically relates the wind stress (τ) to SST anomaly fields (Zhang et al., 2005). The τ field was constructed from an SVD (singular value decomposition) of the covariance matrix that was calculated from the time series of observed monthly anomalies of SST, zonal, and meridional wind stress components during the period of 1963–1996. To achieve reasonable amplitudes, the first five SVD modes were retained in estimating τ fields from SST anomalies.

All coupled model components exchange simulated anomaly fields (Fig. 1). At each time step, the dynamical ocean component produces anomalous ocean pressure, mixed-layer averaged currents, and vertical velocity at the base of the mixed layer (entrainment). Then, from the SL anomaly, a T_e anomaly is calculated with the EOF-based T_e model, serving as an interface between the SST anomaly and dynamical model components. The SST anomaly model then takes the T_e and ocean circulation fields (prescribed mean and simulated), and the observed climatologies of mean SST and vertical temperature gradient to update the SST anomaly. The resultant SST anomaly is then used to calculate wind stress anomalies with the SVD-based τ model. These are then used to force the dynamical ocean model on the next time step. Information between the atmosphere (τ) and the ocean (SST) is exchanged once a day, and the T_e anomalies for the SST anomaly model are also updated once a day from the SL anomalies.

2.2 Initialization schemes

An EnKF data assimilation system for initializing the ICM was first developed by Zheng et al. (2006) and Zheng et al. (2007). In the system, the EnKF is implemented by using an ensemble square-root filter algorithm with no perturbation of observations (e.g., Evensen, 2004). This EnKF data assimilation scheme was further improved by using a balanced, multivariate model-error approach (Zheng and Zhu, 2008) and was upgraded to use mean preserving transformations in the square-root scheme (Sakov and Oke, 2008; Evensen, 2009). The observed interannual SST and SL anomalies can then be consistently assimilated into the coupled model to provide an accurate initial condition for real-time SST prediction (Zheng and Zhu, 2010). In this study, we performed three initialization schemes to isolate the effects of the various initial states on ENSO prediction (Table 1). The first scheme, which is known as Assim_SST, assimilates only the observed SST anomalies into the ICM during the initialization process. In the second scheme, referred to as Assim_SL, the model states of the ICM are periodically updated by assimilating only the SL anomaly data by using EnKF. Moreover, both the SST and SL observations are assimilated into the coupled model to initialize the ICM for the ENSO forecast by using the Assim_SST + SL scheme.

As previously mentioned, the ICM is formed by coupling the ocean model to a simple statistical atmospheric model for interannual wind stress anomalies (τ), and the atmospheric state is a slave only to the modeled SST based on the SVD τ model. Therefore, assimilation of SST observations can provide an accurate initial surface thermal state of ICM and supply a better estimation of the initial atmospheric state. Thus, the Assim_SST scheme in this study represents a better initialization scheme of the surface model states of ICM (Zheng et al., 2006). As described in Sect. 2.1, a distinguished feature added to the dynamical ocean model of ICM for a better performance of SST simulation in the equatorial Pacific is an empirical parameterization for T_e. Observations and modeling studies indicate that variations in SL and the thermocline are well correlated over the equatorial Pacific (e.g., Wyrtki, 1975; Wang and McPhaden, 2000). As such, subsurface temperature anomalies associated with thermocline displacements are closely related with SL variability, which provides a statistical basis for inferring subsurface temperature anomalies from SL variability. Moreover, T_e can be directly estimated from the modeled SL anomalies by the EOF T_e model developed from the historical relationship between the interannual variations in T_e and SL. Thus, assimilation of SL data can directly improve the accuracy of the subsurface thermal state (T_e) of ICM (Zheng et al., 2007), and the Assim_SL scheme represents a better initialization of the subsurface model states of ICM. The Assim_SST + SL scheme is the best initialization scheme of the three different schemes because it can perfect both the surface and subsurface initial states for ICM to provide an ENSO forecast (Zheng and Zhu, 2008). Moreover, to further quantify the relative effects of the accuracy of the surface and subsurface initial states on the 2006–2007 El Niño predictions, the forecast differences between the two single-observational initialization schemes, Assim_SST and Assim_SL, and the double-observational initialization scheme, Assim_SST + SL, were examined to illustrate the relative contributions of the various initial states to ENSO prediction.

2.3 Data sets

The observed monthly SST anomaly fields were from the extended reconstructed SST (ERSSTv3b; Smith et al., 2008), and the monthly-averaged altimeter products were produced by Ssalto/Duacs and were distributed by Aviso, with support from Cnes (http://www.aviso.oceanobs.com/duacs/). Both of the SST and SL data were assimilated into the coupled model once a month, and the SST data were also used to verify the model predictions.

Table 1. Summary of the initialization scheme design.

Initialization scheme	Assimilated data		Description
	SST	SL	
Assim_SST	√		Optimizing the initial surface conditions (i.e., SST and wind stress)
Assim_SL		√	Updating the initial subsurface states (i.e., SL and T_e)
Assim_SST + SL	√	√	Improving the accuracy of both the initial surface and subsurface states

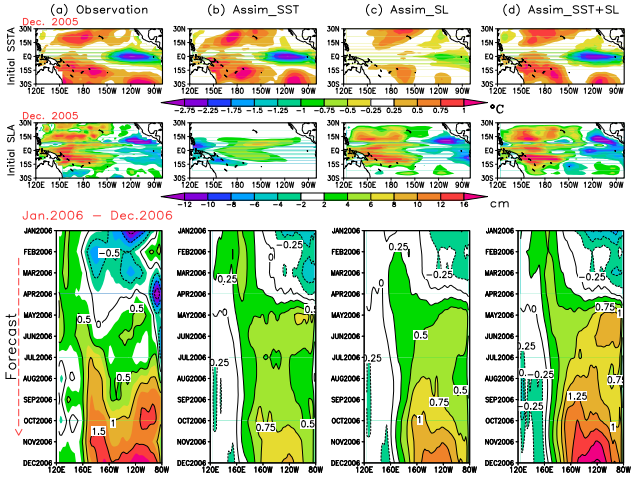

Figure 2. Initial conditions of anomalous SST (top row), SL (middle row), and forecasted SST anomalies (bottom row) from the **(a)** observations, **(b)** Assim_SST results, **(c)** Assim_SL results, and **(d)** Assim_SST + SL results, respectively. The initial fields are from December 2005, and the 12-month forecasts start in January 2006.

3 Isolating the impact of oceanic initial conditions on predicting the 2006–2007 El Niño

We initialized the coupled forecasts of the 2006–2007 El Niño event with the three oceanic analyses on 1 January 2006, and all forecasts had the same atmospheric initial condition. Thus, the outcome depended on the effectiveness of the oceanic initial condition for predicting the 2006–2007 El Niño. The initial conditions of anomalous SST and SL from the Assim_SST, Assim_SL, and Assim_SST + SL analysis results are compared with the observations in the top and middle rows in Fig. 2. As expected, for both the amplitude and spatial pattern of the observed SST, the Assim_SST scheme had a better analysis result than the Assim_SL scheme. However, the Assim_SL scheme had a much more similar assimilation result to the observed SL anomaly field than the Assim_SST scheme. Overall, the Assim_SST + SL scheme had a more reasonable analysis result in both the SST and SL and can provide a more dynamically consistent initial condition for both the surface and subsurface states (Zheng and Zhu, 2008).

The SST hindcasts are also compared with observations in Fig. 2. After initialization, all three hindcasts developed a warm anomaly event during the entire 12 months of the forecast. All of the hindcast experiments with the three different initial conditions successfully predicted the 2006–2007 El Niño event before 12 months, and the hindcast initialized by the Assim_SST + SL scheme performed best. The Assim_SST + SL hindcast exhibited a more realistic evolution during the developing and maturing stages of this El Niño and had the earliest and largest warming of the three experiments, with the first warming in June 2006 and a peak anomaly in December 2006. Moreover, this hindcast had a similar magnitude to the observed warming. The hindcast initialized from the Assim_SL analysis predicted a slightly weaker warming development of the event. Its peak anomaly was approximately 1.3 °C, weaker than that in the Assim_SST + SL forecast and in the observed SST. With the Assim_SST analysis, the warm anomaly developed much slower than the prediction initialized by the Assim_SL analysis or the Assim_SST + SL analysis. For example, in the Assim_SST hindcast, it takes 12 months for the forecasted SST anomalies increasing from 0.2 to 1.0 °C; while in the Assim_SL hindcast, it takes 11 months for the forecasted SST anomalies increasing from 0.2 to 1.3 °C; and in the Assim_SST + SL hindcast, it also takes 12 months for the forecasted SST anomalies increasing from 0.2 to 2.0 °C. The peak anomaly of the Assim_SST hindcast was the weakest among the three hindcast experiments.

When sea level data are assimilated, one major concern is how to project the surface information downward to subsurface layers (Fu and Zhu, 2011). Currently, satellite altimetric observations are assimilated into the coupled general circulation models (CGCMs) or oceanic general circulation models (OGCMs), either by projecting the surface signal to the subsurface due to the statistical relationships between SLA (SL anomalies) and subsurface temperatures (e.g., Fischer et al., 1997; Ji et al., 2000; Masina et al., 2001) or by the inherent multivariate relation derived from the ensembles in order to provide a straightforward way to assimilate SL data through some ensemble-based data assimilation methods (e.g., Oke et al., 2008; Counillon and Bertino, 2009). In this work, similar to the work of Fischer et al. (1997), the relationship between SLA and subsurface thermal state (T_e) is prescribed in a statistical EOF SL-T_e model, and the assimilated anomalous

SL information can be directly projected onto the anomalous subsurface temperature fields of the ocean. Then, the updated subsurface temperature will act to improve the accuracy of the SST prediction during the following forecast process (Zheng et al., 2007).

To illustrate the effect of ocean assimilation performance on the prediction skill for the 2006–2007 El Niño event, the differences between the three forecasts are shown in Figs. 3 and 4. In terms of the observed development of the warm event, the prediction was best when assimilating both the SST and SL observations into the coupled model, Assim_SST + SL. Therefore, the forecast differences between the two single-observational initialization schemes, Assim_SST and Assim_SL, with the double-observational initialization scheme, Assim_SST + SL, can help to isolate the relative effects of the accuracy of the surface and subsurface initial states on the 2006–2007 El Niño predictions.

Figure 3 shows the initial and forecast differences estimated between the Assim_SST + SL and Assim_SL forecasts for SST, zonal wind stress (τ_x), SL, and T_e, illustrating the effects of the initial surface states, SST and wind stress, on predicting the 2006–2007 El Niño event. For the initial period, a more reasonable zonal SST gradient was captured by assimilating the SST observational data into the model in which the SST is anomalously warm west of the dateline and cold to the east (Fig. 3a). This type of zonal SST gradient is convenient for generating stronger westerly winds over the equatorial Pacific (Fig. 3b) at the initial time, which results in the triggering of a considerable El Niño event. As indicated by the SL anomalies (Fig. 3c), the strong westerly wind stress anomalies in the lower atmosphere initiated an oceanic downwelling Kelvin wave, which has been alluded to as a facilitator of El Niño (Picaut et al., 2002; Hackert et al., 2007). Forced by the downwelling Kelvin wave, warm water accumulated in the western Pacific tended to sink and began to propagate eastward, resulting in a net warming at the subsurface layers in the eastern equatorial Pacific during the first half of 2006 (Fig. 3d). When the subsurface warm water reached the eastern tropical Pacific and warmed the surface water through vertical mixing in summer 2006, the warm SST activated the local coupled air–sea interactions to produce atmospheric–oceanic anomalies that developed and evolved with continuous warming during fall 2006. Finally, a 0.4 °C warmer El Niño condition at the end of 2006 was predicted when considering the accuracy of the initial surface ocean–atmosphere condition.

Similarly, the initial and forecasted differences estimated between the Assim_SST + SL and Assim_SST forecasts for SL, T_e, SST, and τ_x are shown in Fig. 4, illustrating the effects of the initial subsurface states, SL and T_e, on prediction of the 2006 El Niño event. Different from the discrepancy induced by the initial surface conditions, the Assim_SST + SL hindcast had an obviously stronger variation in SL than that of Assim_SST, which is associated with the propagation of two downwelling Kelvin waves during the forecast process.

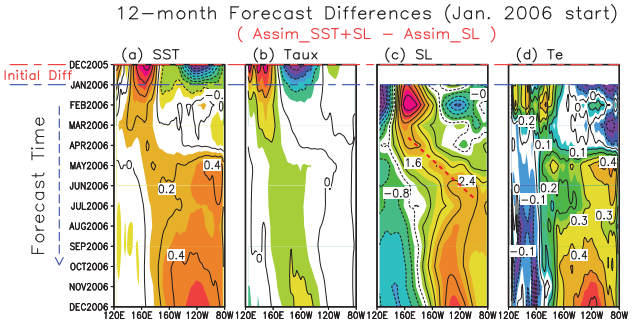

Figure 3. Initial and forecasted differences between the Assim_SST + SL hindcast and the Assim_SL hindcast for **(a)** SST, **(b)** zonal τ_x, **(c)** SL, and **(d)** T_e, illustrating the effects of the initial surface states, SST and τ on predicting the 2006–2007 El Niño event. The dashed red line in **(c)** represents the propagation of the downwelling Kelvin wave. The contour interval is 0.2 °C in **(a)**, 0.08 dyn cm^{-2} in **(b)**, 0.8 cm in **(c)**, and 0.1 °C in **(d)**. The initial differences in December 2005 for the surface states (SST and τ) are demonstrated in the left two panels.

As shown in Fig. 4c and b, the early warming at both the surface and subsurface layers over the eastern equatorial Pacific in the Assim_SST + SL hindcast corresponds to a weak Kelvin downwelling wave initiated east of the dateline before 2006 (Fig. 4a). An additional stronger Kelvin downwelling wave propagated eastbound in approximately January 2006 in the equatorial western Pacific (Fig. 4a, b) and reached the eastern tropical Pacific in mid-2006. These two eastward downwelling propagations resemble the observed events and agree with the timing of the large deepening anomalies of the thermocline depth in the equatorial eastern Pacific (not shown), the details of which have been reported by Hackert et al. (2007). Finally, a 0.8 °C warmer El Niño condition at the end of 2006 was predicted when considering the accuracy of the initial subsurface condition; additionally, much stronger coupled air–sea interaction and vertical mixing induced by the SL assimilation were evident during the second half of 2006 when compared to those induced by the SST assimilation.

As a result, the inclusion of more reasonable and accurate initial conditions during the 2006–2007 El Niño forecast process can lead to better predictions. Figure 5 compares the hindcasts initiated from the three initialization schemes for the 2006–2007 El Niño episode. The hindcasts initialized by the Assim_SST + SL scheme could successfully predict the onset, development, and decay of the 2006 El Niño at all times prior to the event, although some small errors remained in the onset and magnitude of the 2006–2007 El Niño event when forecasted 9 months ahead. The hindcasts initialized by the Assim_SL scheme did not perform as well as those initialized by the Assim_SST + SL scheme; however, they excelled over the those initialized by the Assim_SST scheme. The hindcasts initialized by the Assim_SST scheme diverged

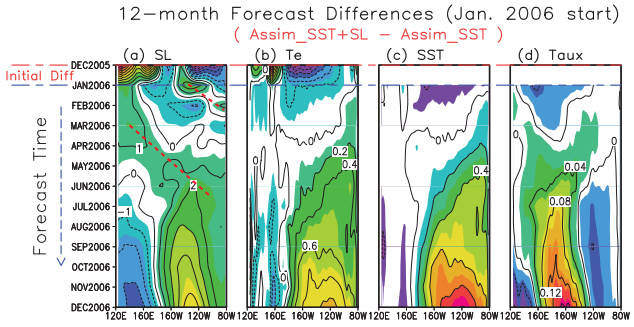

Figure 4. Initial and forecasted differences between the Assim_SST + SL hindcast and Assim_SST hindcast for **(a)** SL, **(b)** T_e, **(c)** SST, and **(d)** zonal τ_x, illustrating the effects of the initial subsurface states, SL and T_e on predicting the 2006–2007 El Niño event. The dashed red line in **(a)** represents the propagation of the downwelling Kelvin wave. The contour interval is 1.0 cm in **(a)**, 0.2 °C in **(b)** and **(c)**, and 0.04 dyn cm^{-2} in **(d)**. The initial differences in December 2005 for the subsurface states (SL and T_e) are demonstrated in the two panels on the left.

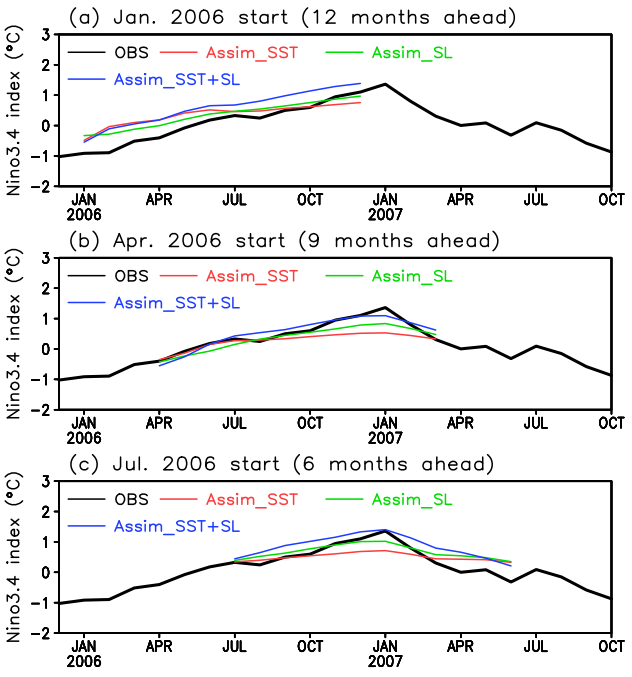

Figure 5. Comparisons of the hindcast results for the 2006–2007 El Niño event. The thick black curves are the observed Niño 3.4 SST anomalies, and the thin curves of red, green, and blue are the predictions initialized by the Assim_SST + SL, Assim_SST, and Assim_SL assimilation results, respectively. **(a)**, **(b)**, and **(c)** are hindcasts that started 12, 9, and 6 months, respectively, ahead of the peak of the 2006–2007 El Niño event.

more obviously from the actual observations when using 12-, 9-, and 6-month time points ahead of the event. However, all of these hindcasts were able to predict the development and decay trend of the event with little departure from the observations. Our methodology of isolating the roles of the initial oceanic states reproduced all of the major features of the 2006–2007 El Niño event. The successful prediction of this event demonstrates that benefits are gained from both the corresponding initial surface and subsurface conditions, although the initial subsurface conditions were more effective.

4 Concluding remarks

The IRI composite forecast table for the December 2006 validation showed that, in general, the amplitude of this 2006–2007 El Niño event was under-predicted by more than 0.5 °C prior to September 2006. By that time, warming in the east should have naturally triggered the dynamical and statistical coupled models to predict El Niño through Bjerknes feedback (McPhaden, 2008). That is, the models were deficient and began to predict El Niño only after the warming in the eastern Pacific had commenced. The results in this study demonstrate the unique ability of data assimilation on improving the initial ocean states to show warming in the coupled system 12 months prior to the event.

Moreover, the impact of the initial details in surface and subsurface states estimated from oceanic data assimilation on coupled forecasts of the 2006–2007 El Niño event was investigated and was isolated in this study. The conceptually simple technique of isolating the role of the initial ocean state through determining the differences in pairs of initialization experiments has been shown to increase the accuracy prediction of the 2006–2007 El Niño. This study further demonstrated that for the 2006–2007 El Niño event, the forecast skill is more significantly affected by the initial state of the subsurface field than by that of the surface field (Zheng et al., 2007; Zheng and Zhu, 2008), suggesting that advanced data assimilation methodology combined with accurate subsurface information should be used in conjunction with coupled forecasts to extend the lead time and accuracy of ENSO forecast systems (e.g., Zhu et al., 2012). Analysis of the results show that the initial conditions having optimal subsurface structures such as SL and T_e fields from the EnKF analysis mainly contributed to improving the intensity prediction in the growth of the 2006–2007 El Niño, although an accurate initial surface state such as SST or wind stress fields can help to easily trigger a warming tendency for predicting the 2006–2007 El Niño event.

Until now, initializing an ENSO-coupled model had mostly focused on generating more realistic ocean surface and subsurface initial states by advanced data assimilation methods (e.g., Alves et al., 2004; Behringer and Xue, 2004; Cazes-Boezio et al., 2010; Vidard et al., 2010). And the assimilation of subsurface temperature observations has been demonstrated to lead to improved forecasts (e.g., Ji and Leetmaa 1997; Zhu et al., 2012). However, over the tropical Pa-

cific Ocean, the distribution of the subsurface data in space and time is quite irregular and sometimes very sparse, even Argo profiles have become available since the 2000s (Balmaseda and Anderson, 2009). Previous works indicated that the assimilation of SL anomalies yields comparable results to the case in which subsurface temperature anomalies were assimilated (e.g., Segschneider et al., 2001). Thus, an alternative data type is given by SL observations due to the availability of the altimetry data in near-real time and the advantage of high spatiotemporal resolution. In this work, we investigated the potential impact of SL assimilation on ENSO forecasts in the 2006–2007 El Niño case. The subsurface thermal state (T_e) can be directly updated by the assimilated SL anomalies through a pre-established statistical EOF SL-T_e model. At the same time, uncertainties in the parameterization of entrainment and vertical mixing continue to lower the SST prediction skill in most state-of-the-art CGCMs (e.g., Latif et al., 2001; Zhang et al., 2005). Our results indicate that there is substantial potential for improving ENSO prediction by minimizing the uncertainties of parameterizing subsurface thermal effects, from projecting the observed SL anomaly information onto subsurface layers based on the statistical relationship.

It should be noted that this work is limited to only one event, and it is difficult to make generic statements about all El Niño events. However, the conceptually simple and robust, technique used here will help coupled models to isolate the role of the initial state of the ocean and to evaluate the conditions favorable for improving El Niño predictions.

Acknowledgements. The authors wish to thank two anonymous reviewers for their helpful comments. This work was supported by the National Program for Support of Top-notch Young Professionals, the National Basic Research Program of China (grant no. 2012CB955202), the Chinese Academy of Sciences (WPOS: XDA10010405) project: Western Pacific Ocean System: Structure, Dynamics and Consequences.

Edited by: D. Stevens

References

Alves, O., Balmaseda, M., Anderson, D., and Stockdale, T.: Sensitivity of dynamical seasonal forecasts to ocean initial conditions, Q. J. Roy. Meteor. Soc., 130, 647–668, 2004.

Ashok, K. and Yamagata, T.: Climate change: The El Niño with a difference, Nature, 461, 481–484, 2009.

Balmaseda, M. A. and Anderson, D.: Impact on initialization strategies and observations on seasonal forecast skill, Geophys. Res. Lett., 36, L01701, doi:10.1029/2008GL035561, 2009.

Barnston, A. G., Tippett, M. K., L'Heureux, M. L., Li, S., and DeWitt, D. G.: Skill of real-time seasonal ENSO model predictions during 2002–2011: is our capability increasing?, B. Am. Meteorol. Soc., 93, 631–651, 2012.

Behringer, D. W. and Xue, Y.: Evaluation of the global ocean data assimilation system at NCEP: The Pacific ocean. Preprints, Eighth Symp. on Integrated Observing and Assimilation Systems for Atmosphere, Oceans, and Land Surface, Seattle, WA, Amer. Meteor. Soc., 2.3, 2004.

Cazes-Boezio, G., Menemenlis, D., and Mechoso, C. R.: Impact of ECCO ocean-state estimates on the initialization of seasonal climate forecasts, J.Climate, 21, 1929–1947, 2010.

Counillon, F. and Bertino, L.: Ensemble optimal interpolation: Multivariate properties in the Gulf of Mexico, Tellus A, 61, 296–308, 2009.

Evensen, G.: Sampling strategies and square root analysis schemes for the EnKF, Ocean Dynam., 54, 539–560, 2004.

Evensen, G.: Data Assimilation: The Ensemble Kalman Filter, 2nd Edn., Springer, Berlin, 2009.

Fischer, M., Flugel, M., Ji, M., and Latif, M.: The impact of data assimilation on ENSO simulations and predictions, Mon. Weather Rev., 125, 819–829, 1997.

Fu, W.-W. and Zhu, J.: Effects of sea level data assimilation by ensemble optimal interpolation and 3D variational data assimilation on the simulation of variability in a tropical Pacific model, J. Atmos. Ocean. Tech., 28, 1624–1640, 2011.

Hackert, E., Ballabrera-Poy, J., Busalacchi, A. J., Zhang, R.-H., and Murtugudde, R.: Role of the initial ocean state for the 2006 El Niño, Geophys. Res. Lett., 34, L09605, doi:10.1029/2007GL029452, 2007.

Ji, M. and Leetmaa, A.: Impact of data assimilation on ocean initialization and El Niño prediction, Mon. Weather Rev., 125, 742–753, 1997.

Ji, M., Reynolds, R. W., and Behringer, D. W.: Use of TOPEX/Poseidon sea level data for ocean analyses and ENSO prediction: Some early results, J. Climate, 13, 216–231, 2000.

Jin, E. K., Kinter III, J. L., Wang, B., Park, C.-K., Kang, I.-S., Kirtman, B. P., Kug, J.-S., Kumar, A., Luo, J.-J., Schemm, J., Shukla, J., and Yamagata, T.: Current status of ENSO prediction skill in coupled ocean–atmosphere models, Clim. Dynam., 31, 647–664, 2008.

Keenlyside, N. and Kleeman, R.: Annual cycle of equatorial zonal currents in the Pacific, J. Geophys. Res., 107, 3093, doi:10.1029/2000JC000711, 2002.

Keenlyside, N., Latif, M., Botzet, M., Jungclaus, J., and Schulzweida, U.: A coupled method for initialising ENSO forecasts using SST, Tellus A, 57, 340–356, 2005.

Kirtman, B. P., Shukla, J., Balmaseda, M., Graham, N., Penland, C., Xue, Y., and Zebiak, S. E.: Current status of ENSO forecast skill: A report to the Climate Variability and Predictability (CLIVAR) Working Group on Seasonal to Interannual Prediction, WCRP Informal Report No. 23/01, 31 pp., 2002.

Latif, M., Anderson, D., Barnett, T., Cane, M., Kleeman, R., Leetmaa, A., O'Brien, J., Rosati, A., and Schneider, E.: A review of the predictability and prediction of ENSO, J. Geophys. Res., 103, 14375–14393, 1998.

Latif, M., Sperber, K., Arblaster, J., Braconnot, P., Chen, D., Colman, A., Cubasch, U., Cooper, C., Delecluse, P., Dewitt, D., Fairhead, L., Flato, G., Hogan, T., Ji, M., Kimoto, M., Kitoh, A., Knutson, T., Le Treut, H., L., T., Manabe, S., Marti, O., Mechoso, C., Meehl, G., Power, S., Roeckner, E., Sirven, J., Terray, L., Vintzileos, A., Voß, R., Wang, B., Washington, W., Yoshikawa,

I., Yu, J., and Zebiak, S.: ENSIP: The El Niño simulation intercomparison project, Clim. Dynam., 18, 255–276, 2001.

Levitus, S.: Climatological Atlas of the World Ocean, NOAA Prof. Paper 13, 173 pp. and 17 microfiche, 1982.

Masina, S., Pinardi, N., and Navarra, A.: A global ocean temperature and altimeter data assimilation system for studies of climate variability, Clim. Dynam., 17, 687–700, 2001.

McCreary, J. P.: A linear stratified ocean model of the equatorial undercurrent, Philos. T. R. Soc. Lond., 298, 603–635, 1981.

McPhaden, M. J.: Evolution of the 2006–07 El Niño: The role of intraseasonal to interannual time scale dynamics, Adv. Geosci., 14, 219–230, 2008,
http://www.adv-geosci.net/14/219/2008/.

McPhaden, M. J., Zebiak, S. E., and Glantz, M. H.: ENSO as an integrating concept in earth science, Science, 314, 1739–1745, 2006.

Monterey, G., and Levitus, S.: Seasonal variability of mixed layer depth for the world ocean, NOAA Atlas NESDIS 14, 96 pp., 1997.

Neelin, J. D., Battisti, D. S., Hirst, A. C., Jin, F.-F., Wakata, Y., Yamagata, T., and Zebiak, S. E.: ENSO theory, J. Geophys. Res., 103, 14262–14290, 1998.

Oke, P. R., Brassington, G. B., Griffin, D. A., and Schiller, A.: The Bluelink ocean data assimilation system (BODAS), Ocean Model., 21, 46–70, 2008.

Palmer, T. N.: A nonlinear dynamical perspective on model error: A proposal for non-local stochastic-dynamic parametrization in weather and climate prediction models, Q. J. Roy. Meteor. Soc., 127, 279–304, 2001.

Picaut, J., Hackert, E., Busalacchi, A. J., Murtugudde, R., and Lagerloef, G. S. E.: Mechanisms of the 1997–1998 El Niño–La Niña, as inferred from space-based observations, J. Geophys. Res., 107, 3037, doi:10.1029/2001JC000850, 2002.

Sakov, P. and Oke, P. R.: Implications of the form of the ensemble transformations in the ensemble square root filters, Mon. Weather Rev., 136, 1042–1053, 2008.

Segschneider, J., Anderson, D. L. T., Vialard, J., Balmaseda, M., Stockdale, T. N., Troccoli, A., and Haines, K.: Initialization of Seasonal Forecasts Assimilating Sea Level and Temperature Observations, J. Climate, 14, 4292–4307, 2001.

Smith, T. M., Reynolds, R. W., Peterson, T. C., and Lawrimore, J.: Improvements to NOAA's Historical Merged Land-Ocean Surface Temperature Analysis (1880-2006), J. Climate, 21, 2283–2296, 2008.

Vidard, A., Balmaseda, M., and Anderson, D.: Assimilation of altimeter data in the ECMWF ocean analysis system 3, Mon. Weather Rev., 137, 1393–1408, 2010.

Wang, W. and McPhaden, M. J.: The surface-layer heat balance in the equatorial Pacific Ocean. Part II: Interannual variability, J. Phys. Oceanogr., 30, 2989–3008, 2000.

Wyrtki, K.: El Niño—The dynamic response of the equatorial Pacific Ocean to atmospheric forcing, J. Phys. Oceanogr., 5, 527–584, 1975.

Yang, S.-C., Rienecker, M., ad Keppenne, C.: The Impact of Ocean Data Assimilation on Seasonal-to-Interannual Forecasts: A Case Study of the 2006 El Niño Event, J. Climate, 23, 4080–4095, 2010.

Zebiak, S. E. and Cane, M. A.: A model El NinoSouthern Oscillation, Mon. Weather Rev., 115, 2262–2278, 1987.

Zhang, R.-H., Zebiak, S. E., Kleeman, R., and Keenlyside, N.: Retrospective El Niño forecast using an improved intermediate coupled model, Mon. Weather Rev., 133, 2777–2802, 2005.

Zheng, F. and Zhu, J.: Balanced multivariate model errors of an intermediate coupled model for ensemble Kalman filter data assimilation, J. Geophys. Res., 113, C07002, doi:10.1029/2007JC004621, 2008.

Zheng, F. and Zhu, J.: Coupled assimilation for an intermediated coupled ENSO prediction model, Ocean Dynam., 60, 1061–1073, doi:10.1007/s10236-010-0307-1, 2010.

Zheng, F., Zhu, J., Zhang, R.-H., and Zhou, G.-Q.: Ensemble hindcasts of SST anomalies in the tropical Pacific using an intermediate coupled model, Geophys. Res. Lett., 33, L19604, doi:10.1029/2006GL026994, 2006.

Zheng, F., Zhu, J., and Zhang, R.-H.: The impact of altimetry data on ENSO ensemble initializations and predictions, Geophys. Res. Lett., 34, L13611, doi:10.1029/2007GL030451, 2007.

Zhu, J., Huang, B., Marx, L., Kinter III, J. L., Balmaseda, M. A., Zhang, R.-H., and Hu, Z.-Z.: Ensemble ENSO hindcasts initialized from multiple ocean analyses, Geophys. Res. Lett., 39, L09602, doi:10.1029/2012GL051503, 2012.